J. Fluid Mech. (1996), vol. 320, pp. 163–184

An improvement to the quasi-steady model with application to cross-flow-induced vibration of tube arrays

By S. GRANGER[1] AND M. P. PAÏDOUSSIS[2]

[1]Research and Development Division, Electricité de France, Chatou, France

[2]Department of Mechanical Engineering, McGill University, Montréal, Québec, H3A 2K6, Canada

(Received 31 January 1995 and in revised form 3 March 1996)

A generalization of the quasi-steady theory is proposed, the aim of which is to model the most important unsteady effects neglected by the conventional quasi-steady assumption. Although this generalized model, referred to as the *quasi-unsteady model*, can be applied in a vast range of flow-induced vibration problems, including classical aeroelasticity, it was primarily developed to improve the theoretical prediction of the fluidelastic behaviour of a single flexible cylinder positioned in the midst of an array of rigid cylinders. In this context, it is shown that the previous improvement to the quasi-steady theory proposed by Price & Païdoussis can be considered as a particular case of the quasi-unsteady model. Results obtained with the quasi-unsteady model are compared to experimental data and to solutions from the Price & Païdoussis model; both modal parameter variation with flow velocity and stability diagrams are considered. This comparison shows that the quasi-unsteady model is a clear improvement on Price & Païdoussis' approach, leading to a more reasonable agreement with experimental results and providing refined insights into the physical mechanisms responsible for fluidelastic instability.

1. Introduction

The quasi-steady theory is frequently used in the study of aeroelasticity (Fung 1955) and flow-induced vibrations (Parkinson & Brooks 1961; Parkinson & Smith 1964; Parkinson 1972; Blevins 1990). This theory allows static fluid force coefficients, determined on a stationary body, to be used to estimate the motion-induced dynamic fluid forces on an oscillating body, providing that it is assumed that, at any instant of time, the body is moving with a constant velocity equal to the actual instantaneous value. It is well-accepted, and physically reasonable, that this assumption is valid for high values of reduced flow velocity. (For a body of characteristic length D, oscillating in a flow of characteristic velocity U_0 with a frequency f, the reduced flow velocity is defined as $U_r = U_0/fD$.)

However, in the area of flow-induced vibration of cylinder (tube) arrays in cross-flow, it is well-known that, in contrast to experimental evidence, the strict quasi-steady theory is unable to predict fluidelastic instability of a *single* flexible tube positioned in the midst of an otherwise rigid tube bundle. This difficulty has been overcome by Price & Païdoussis (1984*a*, 1986) who have improved the quasi-steady theory by taking into account a flow retardation effect in the form of a time delay between the cylinder displacement and the resultant change in the fluid forces.

This idea of introducing a time delay in the analysis of the fluidelastic instability of a cylinder array is also shared by other models, not in the framework of quasi-steady theory. The pioneering work of Roberts (1966) and the analytical 'first principles' model of Lever & Weaver (1982, 1986*a*, *b*) provide two examples. By taking into account such a flow retardation effect, both Price & Païdoussis and Lever & Weaver were able to simulate fluidelastic instability of a single degree of freedom (SDOF) tube array, i.e. a single flexible tube vibrating in the lift direction within an otherwise rigid tube array subject to cross-flow. However, although the qualitative agreement of these models with experimental data seems rather satisfactory, the quantitative accordance is not as good (Price & Païdoussis 1984*a*, 1986; Lever & Weaver 1982, 1986; Yetisir & Weaver 1988; Granger, Campiston & Lebret 1993; Price 1993). Furthermore, the physical significance of the flow retardation effect still remains unclear, and different authors have given different interpretations: Price & Païdoussis, similarly to Simpson & Flower (1977), have postulated that the time lag between the tube motion and the resultant change in the fluid forces is due to retardation of the flow approaching the cylinder in the stagnation region, while Lever & Weaver have assumed that a mass flow redistribution occurs which lags behind tube motion due to fluid inertia. Païdoussis & Price (1988) attribute this effect to a time delay associated with reorganization of the viscous wake flow. It is very likely that this variety of interpretations is essentially due to the rather intuitive nature of the arguments used so far to account for a time delay in these models. Consequently, there seems to be a need for refining the theoretical models in order to improve both the agreement with experimental results and our understanding of the flow retardation effect and, more generally, of the basic physical phenomena responsible for fluidelastic instability of SDOF tube arrays (Price 1995).

In the present paper, a generalization of the quasi-steady theory is proposed. This generalized theory has been derived from a novel approach, compared to Price & Païdoussis' model. The main objectives of this development were: (i) to achieve a far-reaching extension of quasi-steady theory which takes into account all the most important unsteady effects neglected under the strict quasi-steady assumption; (ii) to build up this generalized model on firm theoretical grounds, starting from an analysis of the basic equations governing fluid motion; (iii) to reconsider the flow retardation effect and to develop a formal basis in theory for this effect; (iv) to improve the theoretical agreement with experimental data for SDOF tube arrays.

Theory is presented in §2. First, an analysis of the continuity and Navier–Stokes equations is used to develop a model for the fluid forces induced by an impulsive motion of a body subject to cross-flow. Then, the motion-dependent fluid forces on a body undergoing any general motion are derived from this analysis using the convolution integral. Section 3 deals with the application of this theory to SDOF tube arrays. The flow retardation effect is reconsidered in §3.2. In §3.4, the results obtained with this new model are compared to those of Price & Païdoussis' model and to experimental data. Finally, §4 provides some further insights into the physics of the phenomena involved and proposes a conjecture concerning multiple flexible tube arrays, the aim of which is to suggest a direction for future research work.

2. A 'quasi-unsteady' model for motion-dependent fluid forces

In this section, we consider a two-dimensional flow, in the (x, y)-plane, around a rigid body bounded by $\Gamma(t)$, moving in a fluid domain bounded by Γ_0, see figure 1.

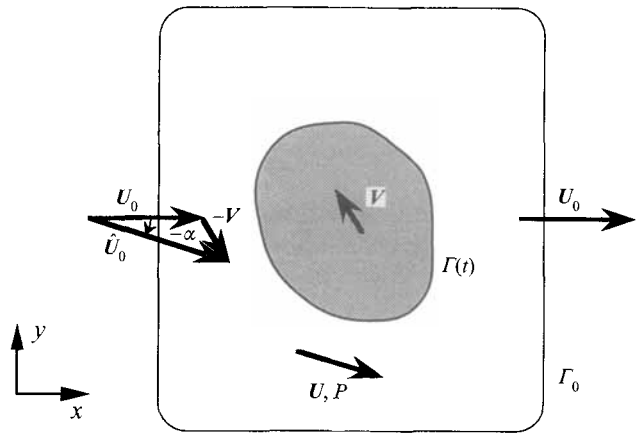

FIGURE 1. Flow around a body moving in a closed fluid domain.

For simplicity, it is supposed that the flow velocity on the Γ_0 boundary is parallel to the x-axis and is denoted by $\boldsymbol{U}_0 = (U_0, 0)^T$; $\boldsymbol{X}(t) = (X, Y)^T$ and $\boldsymbol{V}(t) = (V_x, V_y)^T$ denote the displacement and velocity vectors of the body.

2.1. *Fluid forces induced by impulsive body motion*

It is supposed that the body is at rest for $t < 0$, at a position $\Gamma(0)$, and that it is subjected to a steady flow of velocity $\boldsymbol{U}_1$ and pressure P_1. At $t \geqslant 0$, an impulsive translational movement is imposed on the body,

$$\boldsymbol{V} = \boldsymbol{V}_0 H(t), \quad \boldsymbol{X} = \boldsymbol{V}_0 t H(t), \tag{1}$$

where $H(t)$ is the Heaviside step function. It is assumed that $\boldsymbol{V}_0$ is sufficiently small to allow small-amplitude approximations to be applied. For $t > 0$ the velocity and pressure fields are presumed to be unsteady and will be denoted by $\boldsymbol{U}_2$ and P_2.

The $(\boldsymbol{U}_2, P_2)$ fields are therefore governed by the continuity and *unsteady* Navier–Stokes equations,

$$\nabla \cdot \boldsymbol{U}_2 = 0, \quad \frac{\partial \boldsymbol{U}_2}{\partial t} + \boldsymbol{U}_2 \cdot \nabla \boldsymbol{U}_2 = -\frac{1}{\rho} \nabla P_2 + \nu \nabla^2 \boldsymbol{U}_2, \tag{2a}$$

associated with the boundary conditions

$$\boldsymbol{U}_2 = \boldsymbol{V}_0 H(t) \text{ on } \Gamma(t); \quad \boldsymbol{U}_2 = \boldsymbol{U}_0 \text{ on } \Gamma_0. \tag{2b}$$

On the other hand, the velocity and pressure fields $(\boldsymbol{U}_1, P_1)$ satisfy the continuity and *steady* Navier–Stokes equations, with boundary conditions

$$\boldsymbol{U}_1 = 0 \text{ on } \Gamma(0); \quad \boldsymbol{U}_1 = \boldsymbol{U}_0 \text{ on } \Gamma_0. \tag{3}$$

For this type of problem, frictional forces on the body are considered to be negligible compared to forces due to the pressure. Hence, the fluid forces $\boldsymbol{F}(t)$ acting on the body ($t \geqslant 0$) may be expressed as

$$\boldsymbol{F}(t) = \boldsymbol{F}_0 + \boldsymbol{F}_1(t), \tag{4}$$

where $\boldsymbol{F}_0$ and $\boldsymbol{F}_1$ are the steady and unsteady fluid forces due to P_1 and P_2, respectively. The steady fluid forces may be expressed in terms of dimensionless force coefficients, via

$$\boldsymbol{F}_0 = \tfrac{1}{2} \rho U_0^2 D L \boldsymbol{C}_s, \quad \boldsymbol{C}_s = (C_D, C_L)^T, \tag{5}$$

where D and L are characteristic dimensions of the body in and normal to the (x, y)-plane (e.g. the diameter and length of a circular cylinder); C_D and C_L are, respectively, the steady drag and lift coefficients for the body at its initial position.

In what follows, we shall analyse the evolution of the flow for $t \geqslant 0$, thereby obtaining an analytical model for the unsteady forces $\boldsymbol{F}_1$ induced by the impulsive motion of the body.

Consider first the situation at the onset of movement of the body, i.e. at $t = 0^+$. At $t = 0^+$, the motion-induced flow perturbation is *irrotational*. This is a well-established result about impulsively generated flows (see, e.g., Lamb 1932; Sears 1949; Lighthill 1953; or Batchelor 1967). For the sake of completeness, a quick derivation is given below.

Introducing the difference in flow velocity, $\boldsymbol{u} \equiv \boldsymbol{U}_2 - \boldsymbol{U}_1$, into equations (2) and non-dimensionalizing these equations, order-of-magnitude considerations detailed in Telionis (1981) show that, for $t = 0^+$, equations (2*a*) may be approximated by

$$\nabla \cdot \boldsymbol{u} = 0, \quad \frac{\partial \boldsymbol{u}}{\partial t} \simeq -\frac{1}{\rho} \nabla P_2. \tag{6a,b}$$

Consequently, since $\boldsymbol{u}$ is zero for $t < 0$, equations (6) imply that $\boldsymbol{u}$ is irrotational at $t = 0^+$ and may be expressed in terms of a potential function, ϕ, as $\boldsymbol{u} = -\nabla\phi$.

The velocity–pressure fields $(\boldsymbol{u}, P_2)$ at $t = 0^+$ are thus fully determinable from a solution for ϕ of the Laplace equation. This solution is obtained by taking into account the impermeability condition on the surfaces $\Gamma(0^+)$ and Γ_0:

$$\frac{\partial \phi}{\partial n} \equiv \boldsymbol{u} \cdot \boldsymbol{n} \simeq \boldsymbol{V}_0 \cdot \boldsymbol{n} H(t) \text{ on } \Gamma(0^+); \quad \frac{\partial \phi}{\partial n} \equiv \boldsymbol{u} \cdot \boldsymbol{n} = 0 \text{ on } \Gamma_0, \tag{7}$$

where $\boldsymbol{n}$ is the outward normal on the boundaries.

Lastly, equations (6*b*) and (7) show that the initial irrotational flow perturbation is entirely governed by body acceleration and therefore induces unsteady fluid forces equal to added-mass terms in quiescent fluid. These forces, $\boldsymbol{F}_1^a(t)$, may thus be written as

$$\boldsymbol{F}_1^a = -\tfrac{1}{2} \rho D^2 L \, \mathbf{C}_m \ddot{\boldsymbol{X}}, \tag{8}$$

where $\mathbf{C}_m$ is the matrix of the added-mass coefficients in a quiescent fluid, and $\ddot{\boldsymbol{X}} = \mathrm{d}^2 \boldsymbol{X}/\mathrm{d}t^2$.

Comparison between boundary conditions (7) and (2*b*), (3) shows that at $t = 0^+$ the no-slip condition on the surface of the body is violated in the irrotational flow generated by the impulsive movement. A discontinuity thus exists in the tangential flow velocity on the boundaries of the fluid domain, which may be interpreted, in terms of vorticity, as an infinitely thin layer of vortices distributed on the surface. For $t > 0^+$, boundary layers will develop in the neighbourhood of the surfaces so as to satisfy the no-slip condition, and vorticity will diffuse within these thin layers. In regions of adverse pressure gradient where the irrotational flow reaches zero velocity on the solid boundary, the boundary layer will separate because of viscous friction, which diminishes the kinetic energy of the fluid. Following separation, a portion of the vorticity, initially confined to the boundary layer, will be convected downstream by the flow through large-scale vortices generated by recirculation in the neighbourhood of the separation points. The diffusion–convection process of the vorticity interacts with the initial velocity field, $\boldsymbol{U}_1$, and leads to a fundamental reorganization of the flow, resulting in unsteady fluctuations in the pressure field P_2 for $t > 0^+$. A well-known example of these phenomena is the generation of circulation around an airfoil subject to a real flow (Kundu 1990).

In order to study the influence of movement on the pressure field for $t > 0^+$, equations (2) are recast in terms of a reference frame embedded in the rigid body; writing $\hat{\boldsymbol{U}}_2 = \boldsymbol{U}_2 - \boldsymbol{V}_0$, this leads to (e.g. see Panton 1984):

$$\nabla \cdot \hat{\boldsymbol{U}}_2 = 0, \quad \frac{\partial \hat{\boldsymbol{U}}_2}{\partial t} + \hat{\boldsymbol{U}}_2 \cdot \nabla \hat{\boldsymbol{U}}_2 = -\frac{1}{\rho} \nabla P_2 + \nu \nabla^2 \hat{\boldsymbol{U}}_2 ; \tag{9a,b}$$

$$\hat{\boldsymbol{U}}_2 = 0 \quad \text{on} \quad \Gamma(t); \quad \hat{\boldsymbol{U}}_2 = \hat{\boldsymbol{U}}_0 \equiv \boldsymbol{U}_0 - \boldsymbol{V}_0 \text{ on } \Gamma_0 . \tag{9c}$$

Equations (9) show that the effect of the movement for $t > 0^+$ on the pressure field P_2 is the same as that of a quasi-static displacement of the body subjected to an incident uniform flow of velocity $\hat{\boldsymbol{U}}_0$; thus, for $t > 0^+$, the motion of the body will not generate additional unsteady terms. The unsteadiness of the $(\boldsymbol{U}_2, P_2)$ field will uniquely be due to the flow reorganization following the convection–diffusion of the vorticity produced by the initial movement. It is supposed, therefore, that this reorganization leads to a new steady state after a sufficiently long time, i.e. at $t \gg D/U_0$, as evidenced by an order-of-magnitude analysis of equation (9*b*). Hence, taking both equation (5) and the small-amplitude approximation into account, equations (9) imply that, for $\tau = U_0 t/D \gg 1$, an asymptotic value, $\boldsymbol{F}_1^{\infty}$, of the motion-induced fluid forces, $\boldsymbol{F}_1(t)$, can be expressed as

$$\boldsymbol{F}_1^{\infty} \simeq \tfrac{1}{2} \rho U_0^2 LD \left(\boldsymbol{B} \cdot \overline{\boldsymbol{V}} + \nabla \boldsymbol{C}_s \cdot \overline{\boldsymbol{W}} \right) , \tag{10}$$

where

$$\boldsymbol{B} = \begin{bmatrix} -2C_D & C_L \\ -2C_L & -C_D \end{bmatrix}, \quad \nabla \boldsymbol{C}_s = \begin{bmatrix} \dfrac{\partial C_D}{\partial \bar{x}} & \dfrac{\partial C_D}{\partial \bar{y}} & \dfrac{\partial C_D}{\partial \alpha} \\ \dfrac{\partial C_L}{\partial \bar{x}} & \dfrac{\partial C_L}{\partial \bar{y}} & \dfrac{\partial C_L}{\partial \alpha} \end{bmatrix},$$

$$\overline{\boldsymbol{V}} \equiv \left(\overline{V}_x, \overline{V}_y \right)^T , \qquad \overline{\boldsymbol{W}} = \left(\overline{X}, \overline{Y}, \overline{V}_y \right)^T ;$$

in which α is the apparent angle of attack (figure 1), $\alpha \simeq \overline{V}_y$, and $\overline{X} = X/D$, $\overline{Y} = Y/D$, $\overline{V}_x = V_x/U_0$, $\overline{V}_y = V_y/U_0$; $\bar{x} = x/D$, $\bar{y} = y/D$.

This expression is valid only for $\tau \gg 1$, since the change in the force coefficients is then perturbed by vorticity-induced unsteady effects due to reorganization of the flow. In such a case, equation (10) may be replaced by

$$\boldsymbol{F}_1^{\omega}(t) = \tfrac{1}{2} \rho U_0^2 LD \left[\boldsymbol{B} \cdot \overline{\boldsymbol{V}} + \delta \boldsymbol{C}(\overline{\boldsymbol{W}}) \right] ; \quad t > 0^+ , \tag{11}$$

in which

$$\delta \boldsymbol{C}(\overline{\boldsymbol{W}}) = \left\{ \delta C_{Dx}(\overline{X}) + \delta C_{Dy}(\overline{Y}) + \delta C_{D\alpha}(\overline{V}_y), \, \delta C_{Lx}(\overline{X}) + \delta C_{Ly}(\overline{Y}) + \delta C_{L\alpha}(\overline{V}_y) \right\}^T ,$$

where the terms $\delta C_{kz}(\overline{Z})(k = D, L; \; z = x, y, \alpha; \; \overline{Z} = \overline{X}, \overline{Y}, \overline{V}_y)$ are linear operators (Fung 1955) transforming the input $\overline{Z}(\tau)$, e.g. $\overline{X}(\tau)$, to an output representing the variation of the fluid force coefficient C_k at τ, when $\overline{Z} = \overline{Z}(\tau)$ – the other parameters, e.g. $\overline{Y}$ and $\overline{V}_y$ for $\overline{Z} = \overline{X}$, being kept equal to zero. According to equation (10), the condition

$$\delta \boldsymbol{C}(\overline{\boldsymbol{W}}) \sim \nabla \boldsymbol{C}_s \cdot \overline{\boldsymbol{W}} \tag{12}$$

must be satisfied for an impulsive movement, as $\tau \to +\infty$.

For $z = \alpha$ and $\overline{Z} = \overline{V}_y$, as $\overline{V}_y = \text{constant} = \overline{V}_{0y}$ for $t > 0^+$, in view of equation

(12) we must have

$$\delta C_{k\alpha}(\overline{V}_y) = \frac{\partial C_k}{\partial \alpha}\,\overline{V}_{0y}\,\Phi_{k\alpha}(\tau)\,, \quad \text{with} \quad \lim_{\tau\to+\infty} \Phi_{k\alpha}(\tau) = 1\,. \tag{13}$$

Also, for $z = x, y$ and $\overline{Z} = \overline{X}, \overline{Y}$, if the body displacement is a step function of the type $\boldsymbol{X}(t) = \boldsymbol{X}_0\,H(t)$, then

$$\delta C_{kz}(\overline{Z}) = \frac{\partial C_k}{\partial \overline{z}}\,\overline{Z}_0\,\Phi_{kz}(\tau), \quad \text{with} \quad \lim_{\tau\to+\infty} \Phi_{kz}(\tau) = 1\,. \tag{14}$$

By approximating the real displacement, $\boldsymbol{X}(t)$, by a succession of small steps, applying the principle of superposition and integrating by parts, equation (14) finally leads to

$$\delta C_{kz}(\overline{Z}) = \frac{\partial C_k}{\partial \overline{z}}\,h_{kz} \star \overline{Z}\;; \quad z = x, y\;;\; \overline{Z} = \overline{X}, \overline{Y},\;;\; k = D, L\;; \tag{15}$$

where

$$h_{kz} \star \overline{Z} = \int_0^\tau h_{kz}(\tau - \tau_0)\,\overline{Z}(\tau_0)\,\mathrm{d}\tau_0 \tag{16}$$

is the appropriate convolution integral, and

$$h_{kz}(\tau) = \mathrm{d}\,\Phi_{kz}/\mathrm{d}\tau + \Phi_{kz}(0)\,\delta(\tau), \tag{17}$$

$\delta(\tau)$ being the Dirac delta-function.

Equations (11), (13) and (15) may next be expressed in the Laplace domain, in terms of the Laplace variables s (related to t) and $s_r = sD/U_0$ (related to τ), as follows:

$$\boldsymbol{F}_1^{\omega}(s) = \tfrac{1}{2}\,\rho\,U_0^2\,L\,\boldsymbol{C}_f(s_r)\boldsymbol{X}(s), \tag{18}$$

with

$$\boldsymbol{C}_f(s_r) = s_r\,\boldsymbol{D}_f(s_r) + \boldsymbol{K}_f(s_r),$$

$$\boldsymbol{D}_f(s_r) = \begin{bmatrix} -2C_D & C_L + \dfrac{\partial C_D}{\partial \alpha}\,H_{D\alpha}(s_r) \\ -2C_L & -C_D + \dfrac{\partial C_L}{\partial \alpha}\,H_{L\alpha}(s_r) \end{bmatrix}, \quad \boldsymbol{K}_f(s_r) = \begin{bmatrix} \dfrac{\partial C_D}{\partial \overline{x}}\,H_{Dx}(s_r) & \dfrac{\partial C_D}{\partial \overline{y}}\,H_{Dy}(s_r) \\ \dfrac{\partial C_L}{\partial \overline{x}}\,H_{Lx}(s_r) & \dfrac{\partial C_L}{\partial \overline{y}}\,H_{Ly}(s_r) \end{bmatrix},$$

in which the $H_{kz}(s_r)$ are the Laplace transforms of the $h_{kz}(\tau)$, and $H_{kz}(s_r) = s_r\,\Phi_{kz}(s_r)\;;\; k = D, L\;;\; z = x, y, \alpha$. The inverse transform of equation (18) then allows us to express $\boldsymbol{F}_1^{\omega}(t)$ in the form

$$\boldsymbol{F}_1^{\omega}(t) = \tfrac{1}{2}\,\rho\,U_0^2\,LD(\boldsymbol{D}_f \star \overline{\boldsymbol{V}} + \boldsymbol{K}_f \star \overline{\boldsymbol{X}}), \tag{19}$$

in which

$$\boldsymbol{D}_f(\tau) = \begin{bmatrix} -2\,C_D\,\delta(\tau), & C_L\,\delta(\tau) + \dfrac{\partial C_D}{\partial \alpha}\,h_{D\alpha}(\tau) \\ -2\,C_L\,\delta(\tau), & -C_D\,\delta(\tau) + \dfrac{\partial C_L}{\partial \alpha}\,h_{L\alpha}(\tau) \end{bmatrix}, \quad \boldsymbol{K}_f(\tau) = \begin{bmatrix} \dfrac{\partial C_D}{\partial \overline{x}}\,h_{Dx}(\tau), & \dfrac{\partial C_D}{\partial \overline{y}}\,h_{Dy}(\tau) \\ \dfrac{\partial C_L}{\partial \overline{x}}\,h_{Lx}(\tau), & \dfrac{\partial C_L}{\partial \overline{y}}\,h_{Ly}(\tau) \end{bmatrix},$$

and $\overline{\boldsymbol{X}} = (\overline{X}, \overline{Y})^T$.

A general unsteady model for the fluid forces $\boldsymbol{F}_1$, induced by an impulsive movement of the body, is thus obtained by setting

$$\boldsymbol{F}_1(t) = \boldsymbol{F}_1^{a}(t) + \boldsymbol{F}_1^{\omega}(t), \tag{20}$$

where $\boldsymbol{F}_1^{a}$ is given by equation (8) and $\boldsymbol{F}_1^{\omega}$ is defined by equation (19).

2.2. *Dynamic fluid forces induced by an arbitrary body motion*

For an impulsive movement, equations (8) and (18) show that $\boldsymbol{F}_1$ may be written as a function of $\boldsymbol{X}$ in the following form in the Laplace domain:

$$\boldsymbol{F}_1(s) = \boldsymbol{H}_{FS}(s)\,\boldsymbol{X}(s), \tag{21}$$

in which

$$\boldsymbol{H}_{FS}(s) = -\tfrac{1}{2}\rho D^2 L\,\boldsymbol{C}_m s^2 + \tfrac{1}{2}\rho U_0^2 L\,\boldsymbol{C}_f(s_r).$$

$\boldsymbol{H}_{FS}$ may thus be interpreted as the transfer-function matrix of the linear dynamical system modelling the fluid–structure interaction system. It is well known (Fung 1955; Friedly 1972) that the transfer-function matrix is invariant, whatever the input, $\boldsymbol{X}(s)$. If we consider once more the problem of §2.1, but this time for an *arbitrary* movement of the body, $\boldsymbol{X}(t)$, it is directly evident, therefore, that equations (8) and (18)–(21) apply to an arbitrary movement and hence completely characterize the fluid forces induced thereby. The model thus obtained will be referred to in what follows as *the quasi-unsteady model*, as it constitutes an extension of the quasi-steady model and it accounts for the two types of unsteadiness due to the movement of the body: (i) the forces $\boldsymbol{F}_1^a$, dependent on the acceleration of the movement only and arising from an entrainment effect of the particles in the vicinity of the body, identical to the added-mass effect for a quiescent fluid; (ii) the unsteady component, i.e. the non-quasi-steady one, of the forces, $\boldsymbol{F}_1^\omega$, due to the reorganization of the flow, following the diffusion–convection of the vorticity layer created on the surface of the body after a change in its velocity. The unsteady component of $\boldsymbol{F}_1^\omega$ is characterized by the convolution integrals involving the generalized functions $h_{kz}(\tau)$, with $k = D, L$ and $z = x, y, \alpha$, in equation (19). The h_{kz} terms model the impulse responses of the flow, in terms of the dynamical fluid force coefficients. They are related via equation (17) to the transient functions, Φ_{kz}, representing the evolution of the fluid force coefficient corresponding to step-function changes in displacement or velocity of the body.

2.3. *Transient function modelling*

By setting $h_{kz}(\tau) = \delta(\tau)$, i.e. $\Phi_{kz}(\tau) = H(\tau)$, in equation (19), one recovers from $\boldsymbol{F}_1^\omega$ the quasi-steady theory solution (see, e.g. Blevins 1990). This result is consistent with the fundamental assumption of quasi-steady theory that steady flow is established immediately, as soon as the body has experienced a change in velocity.

In the quasi-unsteady model, the vorticity-induced unsteadiness discussed in §2.1 is accounted for by considering transient functions, $\Phi_{kz}(\tau)$, that evolve continuously towards 1 for $\tau \to +\infty$. They are modelled as follows:

$$\Phi_{kz}(\tau) = [1 - \phi_{kz}(\tau)]\,H(\tau)\ ; \quad k = D, L\ ;\ z = x, y, \alpha\ ; \tag{22a}$$

with

$$\phi_{kz}(\tau) = \sum_{i=1}^{N} \alpha_i\, \mathrm{e}^{-\delta_i \tau}\ , \tag{22b}$$

in which the α_i and δ_i also depend on k and z implicitly.

This modelling can be justified mathematically by invoking Schwartz's theorem stating that any causal continuous function tending to zero as $t \to +\infty$ may be approximated, as closely as desired, by a linear combination of decaying exponentials (Schwartz 1972).

Moreover, a physical argument can be developed from the unsteady aerodynamic theory as follows. Consider the transverse oscillations of a thin airfoil, subject to

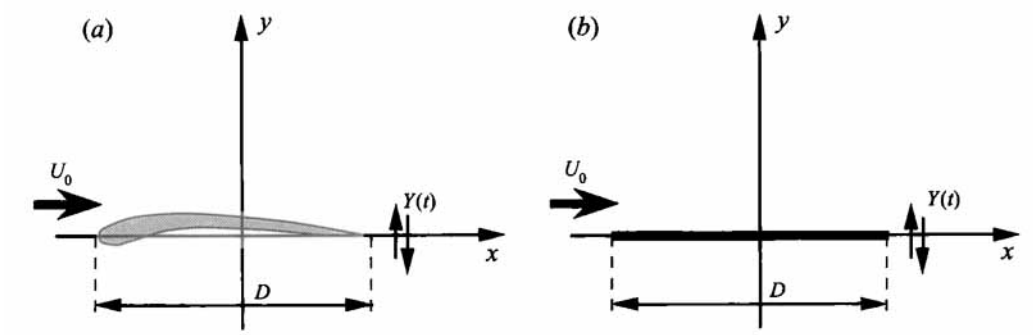

FIGURE 2. A thin airfoil performing vertical-translation oscillations in a two-dimensional incompressible flow: (*a*) the real problem; (*b*) the approximation used in unsteady aerodynamic theory.

an incompressible flow of incident velocity, $\boldsymbol{U}_0$, parallel to the x-axis (see figure 2). Applying the quasi-unsteady theory of §§2.1–2.2 to this problem yields the following expression for the motion-induced fluid force in the y-direction:

$$F_{1y}(t) = -\tfrac{1}{2}\rho D^2 L C_m \ddot{Y} + \tfrac{1}{2}\rho U_0^2 LD\,(\partial C_L/\partial\alpha)\, h_{L\alpha} \star \overline{V}_y, \tag{23}$$

where C_m stands for the coefficient of added-mass in the y-direction. Equation (23) turns out to be identical to the expression derived analytically with the aid of potential flow with singularities, if the transient function, $\Phi_{L\alpha}$, is taken as the Wagner function of unsteady aerodynamic theory (Fung 1955). Furthermore, W.P. Jones has shown that equations (22) with $N = 2$ provide a very good approximation of the Wagner function (Fung 1955). On the other hand, to estimate the fluctuating lift force on a square-section cylinder in transverse oscillation to the oncoming flow, Luo & Bearman (1990) have tentatively applied unsteady aerodynamic theory by modifying the values of the coefficients of added mass, C_m, and of the static-lift derivative, $\partial C_L/\partial\alpha$, to adapt them to their geometry. They thus obtained, for that particular case, an expression formally identical to that of quasi-unsteady theory, in which the transient function $\Phi_{L\alpha}(\tau)$ is modelled by the Wagner function. This model allowed them to improve agreement between theory and experiment, *vis-à-vis* the quasi-steady model of Parkinson (1972) and Parkinson & Smith (1964). Taking into account the differences in the two flows (around a thin airfoil and around a square-section cylinder), Luo & Bearman's results appear to show that the transient function model as suggested by unsteady airfoil theory should have a certain degree of generality and is not a special case applicable only to airfoils.

Admittedly, the expansion defined by equations (22) is not the only possible approximation of the transient functions, $\Phi_{kz}(\tau)$. In some cases, problems may arise, associated with the rate of convergence and the necessary number of decaying exponential terms for a satisfactory approximation. In particular, in the case of oscillatory transients (e.g. transient response of free-surface flows in the context of vibrations of marine structures (Janardhanan, Price & Wu 1992)), the family of decaying exponential functions may judiciously be augmented or replaced by damped sinusoidal functions. Nevertheless, in the following, we have chosen to stay as close as possible to unsteady aerodynamic theory, in view of Luo & Bearman's results. We therefore consider the model defined by equations (22), and we limit ourselves to considering only the first two orders: $N = 1$ and 2. This has the additional advantage of limiting the number of non-dimensional parameters (α_i, δ_i) implicated

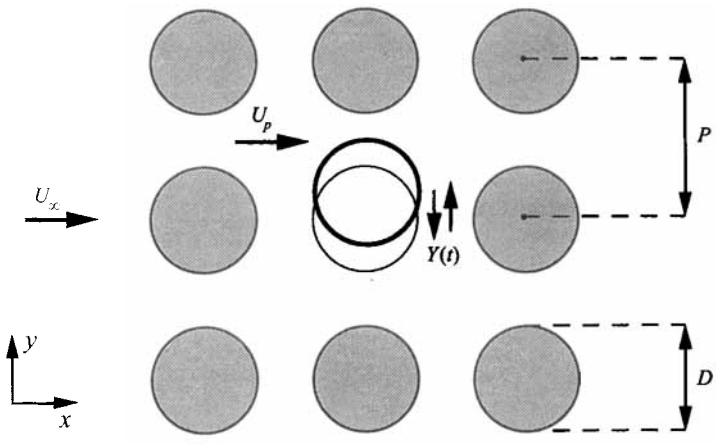

FIGURE 3. A SDOF tube array (square in-line geometry).

in the representation of the unsteady effects associated with the process of diffusion–convection of vorticity.

2.4. *Is the quasi-unsteady model an unsteady model?*

Before closing the theoretical section, it is of interest to make the following point. In the foregoing, it was supposed (cf. §2.1) that the asymptotic behaviour of the flow around a fixed body or one with a constant velocity was steady. When this is not the case, e.g. for a turbulent flow or a flow with vortex shedding, the foregoing theory may nevertheless be applied by considering that the movement of the body generates a perturbation to the mean steady flow. Thus, possible interactions between the motion of the body and the unsteady part of the asymptotic flow are neglected. Although this assumption is not always explicitly stated in the majority of the models for fluidelastic coupling, e.g. in quasi-steady theory (Parkinson 1972; Blevins 1990) and its extensions (Price & Païdoussis 1984*a*; Simpson & Flower 1977), unsteady aeroelasticity (Fung 1955), Lever & Weaver's (1982, 1986*a*, *b*) and Chen's (1987) unsteady models for tube arrays, etc., this assumption is implicitly made in all of them. In these theories, when the unsteady part of the asymptotic flow is taken into account, it is considered as another excitation mechanism, distinct from fluidelastic coupling as such, and described by another model, e.g. as turbulent buffeting excitation or vortex-induced excitation (Blevins 1990; Chen 1987; Corless & Parkinson 1988). The quasi-unsteady model is therefore an unsteady model for fluidelastic coupling, in the sense just defined.

3. Application to SDOF tube arrays

In this section, the quasi-unsteady model is applied to the case of a single flexible cylinder, vibrating in the lift direction, y, in the midst of an array of rigid cylinders subjected to a cross-flow (figure 3). Here, the incident reference flow velocity U_0 is taken to be the interstitial flow velocity $U_p = U_\infty(P/D)/(P/D-1)$, where U_∞ is the velocity upstream of the tube array.

3.1. *Equation of motion of a SDOF tube array*

Taking account of symmetry in this system permits setting $C_L = \partial C_L/\partial\bar{x} = \partial C_D/\partial\bar{y} = \partial C_L/\partial\alpha = \partial C_D/\partial\alpha = 0$, which were confirmed by experiment (Price & Païdoussis

1986). Therefore, according to equations (8), (19) and (20), the fluidelastic force in the y-direction, i.e. the force induced by the movement of the tube on itself, can be expressed as follows:

$$F_{1y}(t) = -\tfrac{1}{2}\rho D^2 L C_m \ddot{Y} + \tfrac{1}{2}\rho U_p^2 LD \left(\frac{\partial C_L}{\partial \bar{y}} h_{Ly} \star \bar{Y} - C_D \bar{V}_y \right), \tag{24}$$

where h_{Ly} is defined by equations (17) and (22).

Hence, denoting by M_s, C_s and K_s the modal mass, damping and stiffness in the mode concerned for vibration in the lift direction, the equation of motion may be written in the Laplace domain as follows:

$$M_e \lambda^2 + C_s \lambda + K_s - \tfrac{1}{2}\rho U_p^2 L \left(\frac{\partial C_L}{\partial \bar{y}} H_{Ly}(\lambda_r) - C_D \lambda_r \right) = 0, \tag{25}$$

for a flow velocity U_p, in which λ is the eigenvalue of the coupled fluid–structure system; $M_e = M_s + \frac{1}{2}\rho D^2 L C_m$ and $\lambda_r = \lambda D/U_p$. The value of λ is related to the eigenfrequency, $\omega(U_p)$, and modal damping coefficient, $\zeta(U_p)$, of the mechanical system under flow conditions by

$$\lambda = -\zeta\omega + \mathrm{j}\omega(1+\zeta^2)^{1/2}, \tag{26}$$

where $\mathrm{j} = \sqrt{-1}$.

Taking into account equations (22), equation (25) may be re-written in the following dimensionless form:

$$\left(\frac{\lambda_r}{\omega_{r0}}\right)^2 + 2\zeta_0 \left(\frac{\lambda_r}{\omega_{r0}}\right) + 1 - \frac{1}{2 m_r \omega_{r0}^2} \left[\frac{\partial C_L}{\partial \bar{y}} \left(1 - \lambda_r \sum_{i=1}^{N} \frac{\alpha_i}{\lambda_r + \delta_i} \right) - C_D \lambda_r \right] = 0, \tag{27}$$

where $\omega_{r0} = \omega_0 D/U_p$, $\omega_0 = (K_s/M_e)^{1/2}$, $\zeta_0 = C_s/2 M_e \omega_0$, $m_r = M_e/\rho D^2 L$.

Equation (27) may be utilized as a basis for (i) estimating the parameters (α_i, δ_i) of the quasi-unsteady model from a 'reference dynamical test' (see §3.3), and (ii) for predicting the fluidelastic behaviour of any SDOF tube array, once the parameters (α_i, δ_i) have been determined (see §3.4). Before illustrating these points, the quasi-unsteady model for SDOF tube arrays will be compared to Price & Païdoussis' model and the problem of the flow retardation effect will be reconsidered.

3.2. *Time delay versus memory effect*

The single-degree-of-freedom (SDOF) model of Price & Païdoussis (1986) can be retrieved from equation (24) by setting $h_{Ly}(\tau) = \delta(\tau - \mu)$, where μ is the non-dimensional time delay introduced by Price & Païdoussis to improve quasi-steady theory. The transient function representing the evolution of the lift coefficient as a result of a step-function change in the y-direction displacement is thus modelled as a lagged Heaviside step-function, i.e. $\Phi_{Ly}(\tau) = H(\tau - \mu)$. Consequently, according to the Price & Païdoussis model, the flow will not respond to a step-change in displacement for $\tau < \mu$; it will attain instantaneously its steady state at time $\tau = \mu$. Physically, this behaviour does not appear to be too realistic and one would rather expect a continuous evolution of the lift coefficient during the transient phase as modelled by equations (22). As seen in §2.1, this evolution is basically due to the fact that a change in the velocity of the cylinder induces on its surface a thin vorticity layer, which is later diffused into the boundary layer and then transported downstream by the mean flow. This phenomenon eventually leads to an unsteady perturbation in the velocity and pressure fields in the neighbourhood of the cylinder, which decays continuously

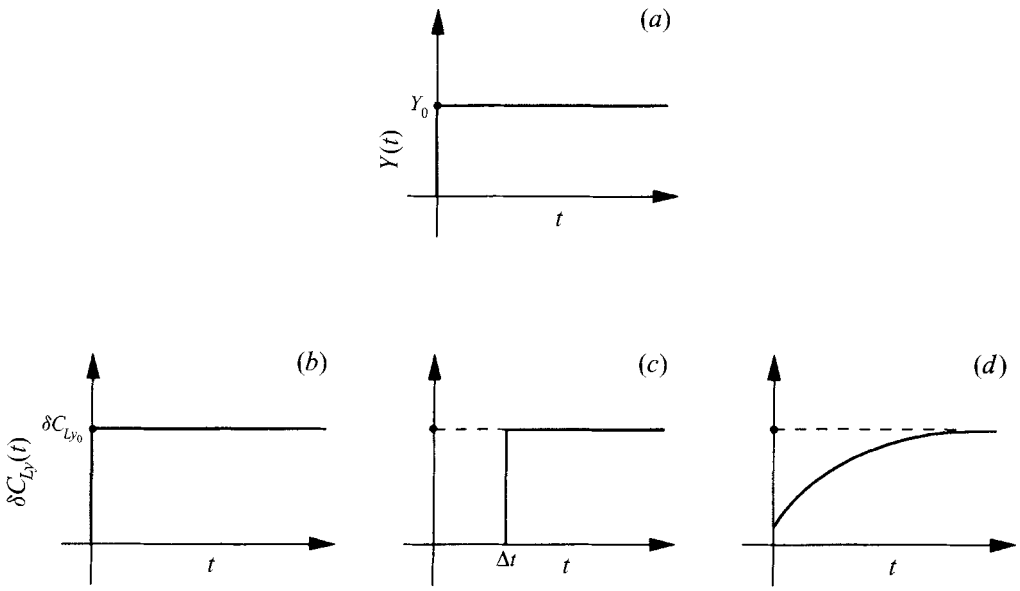

FIGURE 4. Transient variation of lift coefficient, $\delta C_{Ly}(t)$, induced by a step displacement $Y(t) = Y_0 H(t)$: (*a*) $Y(t)$; (*b*) quasi-steady theory; (*c*) Price & Païdoussis model; (*d*) a continuous variation typical of the quasi-unsteady model (order 1), $\delta C_{Ly0} \equiv (\partial C_L/\partial \bar{y})\overline{Y}_0$, $\Delta t = \mu D/U_p$.

with time as the vorticity is convected downstream. In the end, a new steady state is reached, when the motion-induced vorticity has been transported sufficiently far from the cylinder by the mean flow, so that its influence on the pressure at the cylinder surface becomes negligible. This is the physical mechanism modelled by equations (22). Figure 4 shows the different transient behaviour of the lift coefficient for the quasi-steady, Price & Païdoussis, and quasi-unsteady models, respectively.

For an arbitrary movement of the cylinder, as the quasi-unsteady model considers a continuously evolving transient function the convolution integral in equation (24) implies that the motion-induced fluid force depends on the whole past time history of cylinder displacement. This models the fact that, for a general motion, the fluid force at a given instant involves the superposition of vorticity-induced perturbations due to the ensemble of changes in the cylinder velocity at earlier times. In contrast, Price & Païdoussis (1986) assumed that the motion-induced fluid force at time t should depend solely on the particular value of cylinder displacement at time $t - \mu D/U_p$.

Therefore, rather than a delay effect, as previously conceived in the earlier models, the quasi-unsteady model proposes *a memory effect* in the flow, the physical origin of which arises from the diffusion–convection process of the vorticity induced by successive changes in the velocity of the body. This, in retrospect, may also explain why purely potential-flow models are incapable of predicting oscillatory fluidelastic instability (Païdoussis, Mavriplis & Price 1984).

3.3. *Model parameter estimation: an inverse method*

A 'reference dynamical test' is considered, i.e. a dynamical test for a given array geometry in which the flexible tube is free to vibrate under the action of flow. For different flow velocities, the vibratory response of this tube is measured, determining thereby the variation with U_p of the modal parameters ω and ζ. A signal processing method enabling this type of estimate has been described by Granger (1990). For in-

line square and normal triangular arrays, such data have been obtained by Granger *et al.* (1993). The curves $\omega(U_p)$ and $\zeta(U_p)$ enable the determination via equation (26) of a set of values of λ_r, which are solutions of equation (27). The geometrical and dynamical characteristics of the mechanical system being known, so are the parameters ω_{r0}, ζ_0 and m_r. Consequently, if $\partial C_L/\partial \bar{y}$ and C_D are known in advance, the parameters α_i, δ_i, $i = 1, N$, of the quasi-unsteady model may be calculated with equation (27) from a selected set of N values of λ_r, associated with N distinct flow velocities.

In the case of the first-order model ($N = 1$), it is even possible to obtain approximate values of α_1 and δ_1 via equation (27) with just one measurement, that of the critical flow velocity, U_{pc}, i.e. the velocity at which fluidelastic instability occurs in the reference dynamical test. This is achieved by using the identity $\zeta(U_{pc}) = 0$ and the approximation $\omega(U_{pc}) \simeq \omega_o$. This approximation is justified in practice by the weak variation of ω with U_{pc} (see e.g. figures 5 and 6). The following approximate formulae are thus obtained:

$$\delta_1 = \omega_{r0}^2 \left[\frac{-4 m_r \omega_{r0} \zeta_0 - C_D}{\partial C_L/\partial \bar{y}} \right], \qquad \alpha_1 = \frac{\delta_1^2 + \omega_{r0}^2}{\omega_{r0}^2}, \tag{28}$$

in which $\omega_{r0} = \omega_0 D/U_{pc}$.

As described by Price & Païdoussis (1984*a*, *b*), $\partial C_L/\partial \bar{y}$ and C_D may be determined by static tests. For the square in-line array, the data from Price & Païdoussis (1986) will be used, taking into account that they were non-dimensionalized with respect to U_∞. Defining $a = U_p/U_\infty$, for $P/D = 1.5$ and with the notations of this paper we have: $\partial C_L/\partial \bar{y} = -73/a^2$, $C_D = 2.3/a^2$. For the normal triangular array, new tests conducted at McGill University with $P/D = 1.375$ have given $\partial C_L/\partial \bar{y} = -19.2/a^2$, $C_D = 3.8/a^2$.

Choosing therefore a point close to fluidelastic instability in the data of Granger *et al.* (1993), equation (27) gives the estimations

$$\alpha_1 = 1.097, \quad \delta_1 = 0.039 \quad \text{for the square in-line array, and}$$

$$\alpha_1 = 1.418, \quad \delta_1 = 0.141 \quad \text{for the normal triangular array.}$$

For the second-order ($N = 2$) model, equation (27) necessitates knowledge of (ω, ζ) for two points of flow velocity in the reference dynamical test. By utilizing as the first point one close to the onset of fluidelastic instability and the second point roughly half-way in the data of Granger *et al.* (1993), we obtain

$$\alpha_1 = 1.134, \quad \delta_1 = 0.084, \quad \alpha_2 = -0.121, \quad \delta_2 = 1.723,$$

$$\alpha_1 = 2.172, \quad \delta_1 = 0.48, \quad \alpha_2 = -2.684, \quad \delta_2 = 2.72,$$

for the square in-line and normal triangular array, respectively. It is noted that the values of α_1 and δ_1 are not modified too much in going from the model of order 1 to that of order 2 for the square in-line array, which is not the case for the normal triangular array.

3.4. *Theoretical prediction and comparison with experimental data*

With the model parameters determined, equation (27) may be used to predict the dynamical behaviour of a single-degree-of-freedom tube array for any given m_r, ζ_0, ω_0 and D. Thus, the specification of ω_{r0} corresponding to a given value of U_p allows the determination of λ_r, and hence of $\omega(U_p)$ and $\zeta(U_p)$. We may thus predict the variation of the modal parameters ω and ζ as functions of the flow velocity and, via

$\zeta(U_{pc}) = 0$, determine the critical flow velocity, U_{pc}, for the threshold of fluidelastic instability.

Here, the results obtained in this manner will be compared with those of Price & Païdoussis' model and with experimental data. Two types of comparisons are made: one in terms of the variation of $\omega(U_p)$ and $\zeta(U_p)$ for $U_p \leqslant U_{pc}$, and the other in terms of the instability charts of $U_{prc} = U_{pc}/f_s D$ versus the mass-damping parameter $A_r = M_s \delta/\rho D^2 L$, for several geometric configurations (i.e. values of P/D); (δ and f_s here represent the logarithmic decrement and natural frequency (in Hz) of the tube in air). The first type of comparison permits, for a limited number of geometries, the refined analysis of the development of fluid–structure interaction, up to the critical flow velocity. The second type of comparison takes into account but the final result, i.e. fluidelastic instability; however, in view of the large number of geometric configurations that could be compared, it nevertheless allows a global view of the validity of the models.

To ensure that this second type of comparison is reliable, it is necessary that the experimental points appearing in these instability graphs have been analysed in the same way and they correspond to *homogeneous* and *representative* configurations as compared to the system for which the model has been developed, for this latter then to predict a kind of averaged behaviour. For this reason, in the instability graphs, experimental data obtained with only a single flexible cylinder in the midst of a rigid tube array have been considered exclusively. In contrast, among the data selected, some come from direct observation of fluidelastic instability (Price & Païdoussis 1989; Andjelić & Popp 1989; Granger 1990; Granger *et al.* 1993; Lever & Rzentkowski 1993; Nakamura & Fujita 1993), whereas others were obtained *indirectly* from measurements of the fluidelastic forces (Tanaka, Takahara & Ohta 1982; Teh & Goyder 1988). Furthermore, in some cases the tube could only vibrate in the lift direction (Tanaka *et al.* 1982; Teh & Goyder 1988; Lever & Rzentkowski 1993; Nakamura & Fujita 1993), while in others it could also vibrate in the drag direction (Andjelić & Popp 1989; Price & Païdoussis 1989; Granger 1990; Price & Zahn 1991; Lever & Rzentkowski 1993; Granger *et al.* 1993). Two configurations, one for each geometry, were studied and compared in terms of variations of the modal parameters, ω and ζ, as functions of flow velocity. They come from Granger *et al.* (1993) and correspond to a single flexible cylinder centrally located in the midst of a rigid tube array in water flow; they are the same experimental data as those used in §3.3.

The experimental evolution of the modal parameters for the two configurations studied is compared in figures 5 and 6 with those predicted by (*a*) the Price & Païdoussis model and (*b*) the quasi-unsteady model of orders 1 and 2. For the former model the calculations have been conducted with $\mu = 1$, a parametric study having confirmed that the 'best' results were in fact obtained with this value, as previously found (Price & Païdoussis 1984*a*). Figures 5 and 6 show that the predictions by the Price & Païdoussis model are qualitatively correct (the tendency toward lower frequency with increasing U_p and the corresponding increase–decrease in the damping coefficient prior to the onset of instability), but these effects happen much too fast as U_p is increased compared to the experimental behaviour; this leads to an underestimation of the critical flow velocity. It is certainly possible to adjust the value of μ in Price & Païdoussis' model so as to obtain better agreement in the critical flow velocity, but then the qualitative agreement with experiment in the subcritical region, i.e. for $U_p \leqslant U_{pc}$, is lost. It should be noted that similar conclusions have previously been reached with respect to the Lever & Weaver model (Granger *et al.* 1993). In

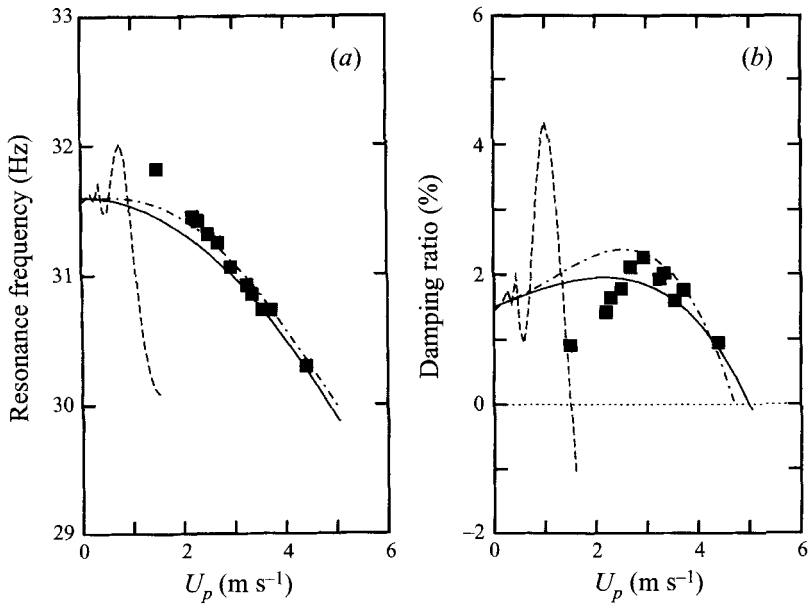

FIGURE 5. SDOF tube array. Results for square in-line geometry in cross-flow showing modal parameter variations with flow velocity: (*a*) resonance frequency and (*b*) modal damping ratio versus U_p. ■, experimental results; – –, Price & Païdoussis model; ——, quasi-unsteady model (order 1); –·–, quasi-unsteady model (order 2).

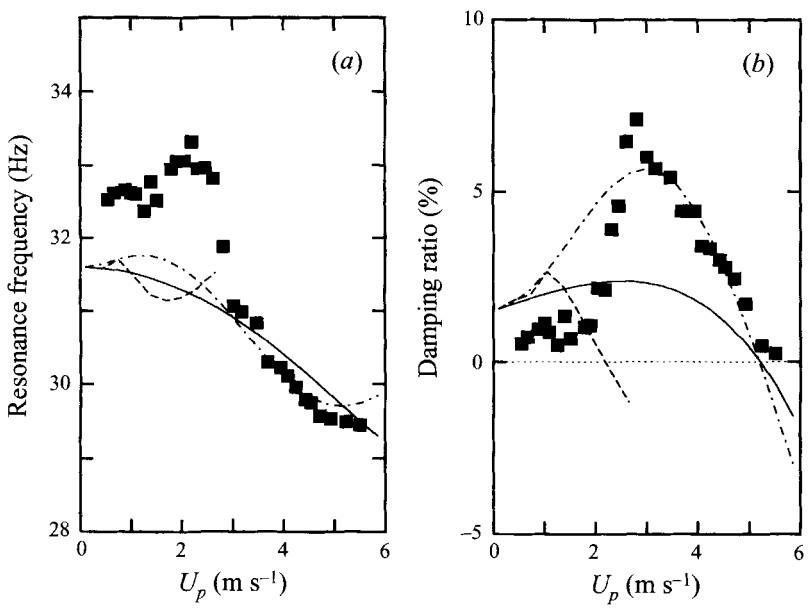

FIGURE 6. As figure 5 but for normal triangular geometry.

contrast, the quasi-unsteady model can yield a correct critical flow velocity, as well as qualitatively satisfactory behaviour in the subcritical zone.

In the case of the square in-line array, there is not a great deal of difference in the results of the order-1 and order-2 quasi-unsteady models. Apart from the qualitative agreement, good quantitative agreement with the experimental data is obtained for

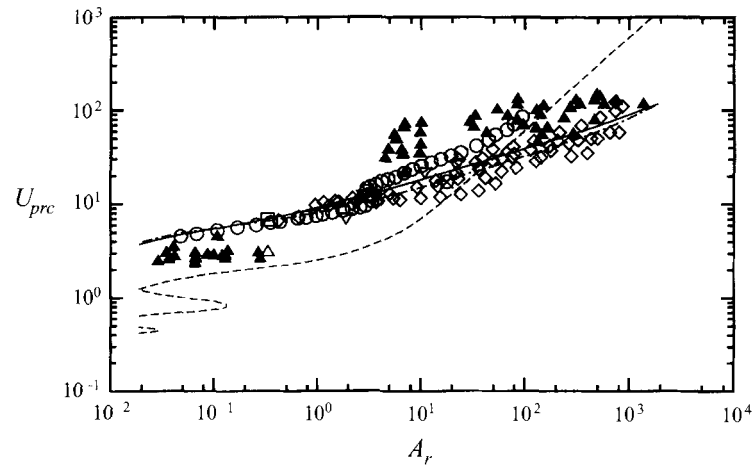

FIGURE 7. Stability map for SDOF tube array. Results for square in-line geometry. Symbols, experimental data: ○, Tanaka *et al.* (1982), $P/D = 1.33$; △, Granger *et al.* (1993), first row, $P/D = 1.44$; □, Granger *et al.* (1993), middle row, $P/D = 1.44$; ▲ Price & Païdoussis (1985), $P/D = 1.5$; ◇, Teh & Goyder (1988), $P/D = 1.35$; ▽, Lever & Rzentkowski (1993), $P/D = 1.433$; ⊗, Nakamura & Fujita (1993), $P/D = 1.40$; – –, Price & Païdoussis model; ——, quasi-unsteady model (order 1); –·–, quasi-unsteady model (order 2).

$U_p \geqslant 2.5$ m s^{-1}; for $U_p < 2.5$ m s^{-1}, however, the quasi-unsteady model tends to overestimate the damping coefficient – even though the predicted values are of the right order of magnitude. For the normal triangular array, the difference between the predictions of the order-1 and order-2 models is more marked. The order-2 quasi-unsteady model yields an evolution which is quantitatively correct for $U_p > 3$ m s^{-1} approximately, whereas the order 1 model tends to underestimate the coefficient of damping by a factor of 3.5 approximately, e.g. 2% instead of 7% at $U_p \simeq 3$ m s^{-1}. For $U_p < 2$ m s^{-1}, both order-1 and order-2 models tend to overestimate the damping coefficient, though the predictions are still of the right order of magnitude.

Figures 7 and 8 show the comparison of the experimental fluidelastic instability data to the predictions of the Price & Païdoussis and quasi-unsteady models for the square-in line and the normal triangular arrays, respectively.

For the square in-line array (figure 7) and $A_r \leqslant 3$, most of the experimental results are mutually coherent, except those of Price & Païdoussis (1989) and that of Granger *et al.* (1993) corresponding to a flexible tube in the front row of the array. These points are clustered around a horizontal straight line, lying below the other points, with $U_{prc} \simeq 2.8$. For $A_r > 3$, the various data of Teh & Goyder (1988), Lever & Rzentkowski (1993) and Nakamura & Fujita (1993) are in good agreement, Price & Païdoussis' data are sensibly higher, while the semi-empirical ones by Tanaka *et al.* (1982) are in between. The results obtained by the quasi-unsteady model of orders 1 and 2 are not very different. They are able to fit well the average trends of the experimental data. If the Price & Païdoussis and the first-row Granger *et al.* experimental data are excluded, the agreement may even be considered to be excellent. The results obtained with the Price & Païdoussis model are not as good.

For the normal triangular array (figure 8), the agreement between experimental data from various sources is very satisfactory for $A_r \leqslant 20$ approximately; beyond that, two types of behaviour, characteristic of the Teh & Goyder (1988) data, on the one hand, and of the Price & Zahn (1991) data, on the other, are found. In this case

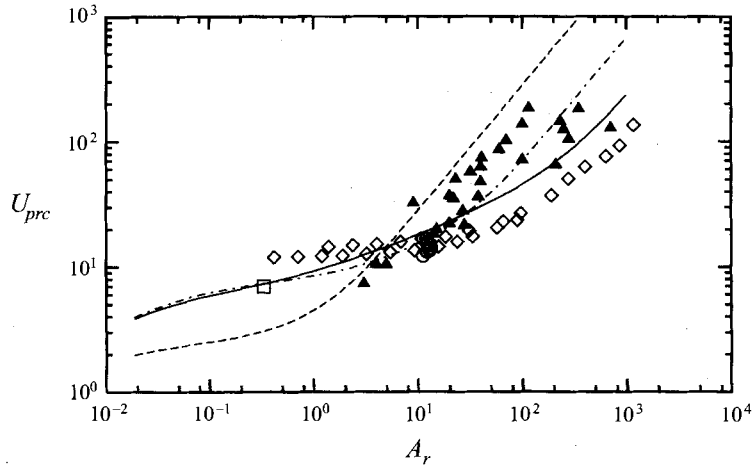

FIGURE 8. Stability map for SDOF tube array. Results for normal triangular geometry. Symbols, experimental data: ○, Andjelić & Popp (1989), $P/D = 1.25$; □, Granger (1990), $P/D = 1.44$; ▲, Price & Zahn (1991), $P/D = 1.375$; ◇, Teh & Goyder (1988), $P/D = 1.35$; – –, Price & Païdoussis model; ——, quasi-unsteady model (order 1); –·–, quasi-unsteady model (order 2).

also, the results obtained by the quasi-unsteady model are superior to those of the Price & Païdoussis model. In this case, however, the difference between the results of the order-1 and order-2 models is substantial for $A_r \geqslant 20$ approximately: whereas the order-1 model gives a curve in between the Price & Zahn and Teh & Goyder data, the curve predicted by the order-2 model is closer to the Price & Zahn data.

In view of these results, it appears that the series representation of the transient function (equations (22)) seems to converge rapidly for the square in-line array, so that order-2 modelling does not yield significantly different results than the order-1 analysis. In contrast, for the normal triangular geometry, it is manifestly desirable to study the results with models of order higher than 2.

4. Discussion

The experimental results presented in the foregoing show that the quasi-unsteady model is an improvement on the model by Price & Païdoussis, which itself is an improvement on quasi-steady theory. This sensibly improved theoretical prediction can be attributed to a better account of unsteady mechanisms in the quasi-unsteady model, as discussed in §3.2. This has been achieved at the expense of a more complex (but also more physical) model for these phenomena, involving a memory effect of the flow rather than the flow retardation effect suggested by the earlier models.

Nevertheless, as pointed out in §2.4, the quasi-unsteady model still does not represent all unsteady effects that may arise when a body is oscillating in a cross-flow. Only the interaction between the body motion and the mean steady flow is taken into account. For example, interactions between motion and periodic vortex shedding are entirely neglected.

This might explain why in the case of square in-line arrays the model reproduced well the upper branch of the instability chart for $A_r \leqslant 0.3$, but not the lower branch corresponding to $U_{prc} \simeq 2.8$ = constant and associated with some of the Price & Païdoussis (1989) and Granger *et al.* (1993) experimental data. In fact, it was shown (Granger *et al.* 1993) that the fluidelastic instability in that case (front-row rather

than central-row tubes) interacted with periodic vortex shedding; this interaction, or interference, was attenuated with increasing turbulence levels deeper in the array. Furthermore, additional data recently obtained at McGill University and analysed at Electricité de France by the same modal identification method as that used previously by Granger *et al.* (1993) have confirmed the Price & Païdoussis results (1989) for $A_r \leqslant 0.3$; although in this case the tube is closer to the centre of the array, these unpublished results show similar behaviour to that in the first row of Granger *et al.* (1993). In particular, fluidelastic instability appears to be influenced by interaction with periodic vortex shedding. Finally, another argument that may be invoked to reinforce this explanation of the behaviour for $A_r \leqslant 0.3$ in the square in-line array is based on the Strouhal number, St, corresponding to the value of $U_{prc} = 2.8$; converted to U_r, this gives $St = 1.07$, which is in very good agreement with the Weaver, Fitzpatrick & El Kashlan (1986) correlation for vortex shedding.

At this stage of the discussion, the following important question has remained unanswered: what happens in arrays of *flexible* tubes? It is recalled that the quasi-unsteady model was purposely developed for the simplified case of a SDOF (single-degree-of-freedom) tube array, involving but one flexible tube, to facilitate the precise analysis of the underlying mechanisms for fluidelastic instability, without the added complications associated with inter-tube coupling. Rigorously, it is clear that further development is necessary in order to model the behaviour of fully flexible arrays. Nevertheless, a number of authors (Weaver & Grover 1978; Weaver & Koroyannakis 1982; Lever & Weaver 1982; Lever & Rzentkowski 1993) have observed, on the basis of experiments in air, that the effect of neighbouring flexible tubes, at least insofar as fluidelastic instability is concerned, is rather weak. Granger *et al.* (1993) have similarly observed in their tests that the critical flow velocity of a flexible array in water cross-flow was close to that of a single flexible tube located in the first row of a rigid-tube array. Moreover, in the case of the flexible array, their results suggest that at the onset of fluidelastic instability there is an interaction with a vortex-shedding phenomenon, similarly to the case of a single flexible tube in the first row of the array. The influence of neighbouring tubes appears to be confined to amplifying the interaction phenomena and to homogenizing them within the array. This observation accords equally well with the instability charts where, for flexible tube arrays, the results cluster about $U_{prc} \simeq$ constant for A_r less than 1 approximately (Weaver & Fitzpatrick 1988).

It has therefore appeared worthwhile to undertake the following exercise: for square in-line, normal triangular and parallel triangular arrays, to compare on the same instability chart (i) the results of the quasi-unsteady model of order 1, (ii) the experimental data assembled by Weaver & Fitzpatrick (1988) for flexible tube arrays, and (iii) the zone of reduced flow velocities corresponding to 'reasonable' Strouhal numbers, obtained from the empirical correlations of Weaver & Fitzpatrick (1988) for pitch-to-diameter ratios in the range P/D =1.3–1.5. For the square in-line and the normal triangular arrays we have used the parameters of the model as determined in §3.3 for SDOF tube arrays. For the parallel triangular geometry, the parameters (α_1, δ_1) of the order-1 quasi-unsteady model were obtained with the aid of the simplified procedure of §3.3 (equation (28)), utilizing Price & Païdoussis' (1986) values of $\partial C_L/\partial \bar{y}$ and C_D and the critical flow velocity of one point in Weaver & Fitzpatrick's (1988) instability chart in the vicinity of $m\delta/\rho D^2 = 2$, where $m = M_e/L$. This gives $\alpha_1 = 1.0$, $\delta_1 = 0.066$. The results are summarized in figure 9. The quasi-unsteady model for SDOF tube arrays compares favourably to experimental data for $m\delta/\rho D^2 \geqslant 3$ for square in-line and normal triangular geometries. Moreover, the

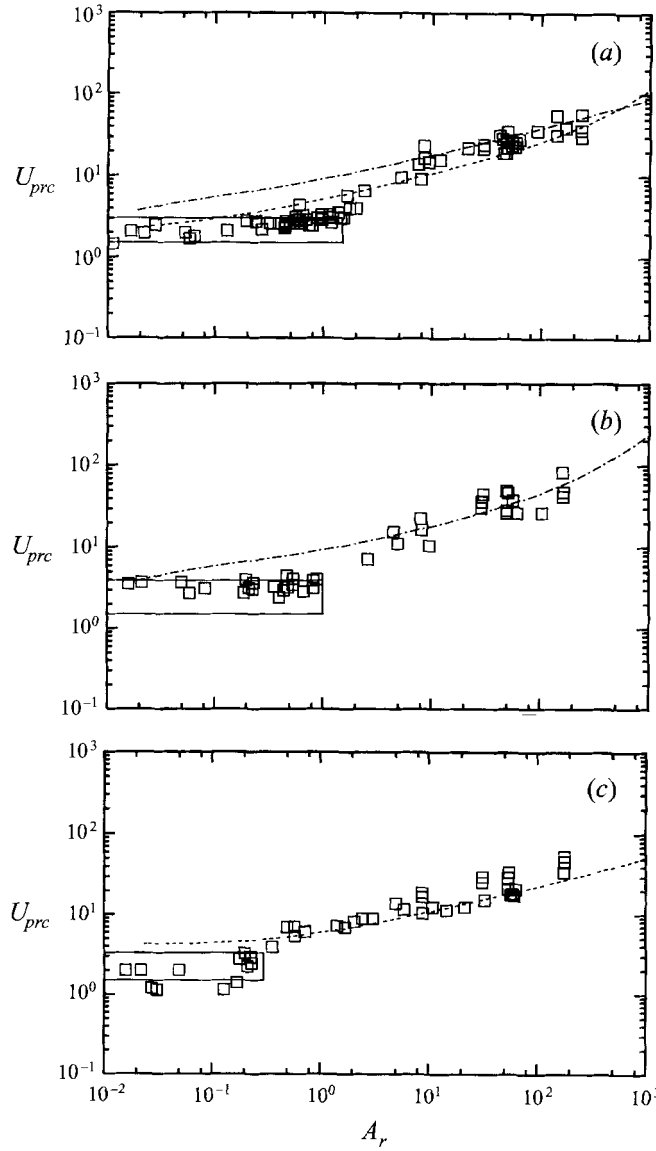

FIGURE 9. Stability maps for flexible tube arrays: (*a*) square in-line geometry; (*b*) normal triangular geometry; (*c*) rotated triangular geometry. Notation: □, experimental data (Weaver & Fitzpatrick 1988); –·–, quasi-unsteady model of order 1 with SDOF tube array parameters; ——, boundary of the region of possible Strouhal excitation, from Weaver & Fitzpatrick (1988); – – –, quasi-unsteady model with parameters determined from one point of the flexible tube array stability map.

procedure adopted for the rotated triangular arrays gives very satisfactory agreement for $m\delta/\rho D^2 \geqslant 0.3$. Interestingly, by adopting a similar procedure, better results may be obtained for the other two array geometries also. This is illustrated in figure 9(*a*), where the results obtained by the quasi-unsteady model of order 1 are also shown, obtained with $\alpha_1 = 1.10$ and $\delta_1 = 0.20$ and all other parameters the same.

Considering small values of $m\delta/\rho D^2$ next, it is noted that for $10^{-2} \leqslant m\delta/\rho D^2 \leqslant 1.5$ for the square in-line geometry, $10^{-2} \leqslant m\delta/\rho D^2 \leqslant 1$ for the normal triangular geometry, and $10^{-2} \leqslant m\delta/\rho D^2 \leqslant 0.3$ for the rotated triangular one, a good correlation

is revealed between the regions of vortex shedding and of fluidelastic instability. The results taken together suggest that for large mass-damping parameter values, i.e. $O(1) \leqslant A_r \leqslant O(10^3)$, inter-tube coupling can have a significant effect (figure 9), but is clearly not the driving mechanism for fluidelastic instability. For low mass-damping parameter values, however, i.e. $A_r \leqslant O(1)$, it would appear that in a similar way as we have just seen for square in-line SDOF tube arrays, there may be a strong interaction between the 'vortex shedding' and 'fluidelastic instability' phenomena. Still, with the present state of knowledge, all this cannot but be conjectural. Nevertheless, the results of figure 9 certainly give a great deal of food for thought and suggest that further work would be useful.

Finally, it will not have escaped the reader that the rotated square array geometry has been left out of this discussion. This is because its behaviour is peculiar and does not follow the pattern of the foregoing. As shown by Païdoussis *et al.* (1989) for instance, a single flexible cylinder in such an array with $P/D = 1.5$ does not develop fluidelastic instability; whereas, if several cylinders are flexible, instabilities can arise, as shown by Price & Kuran (1991). Evidently, a special discussion is required for this geometry, which is beyond the scope of this paper.

5. Conclusion

In this paper, a generalization of quasi-steady theory has been proposed and applied to the case of a flexible tube (cylinder) vibrating in the midst of an array of rigid tubes, submitted to a cross-flow (SDOF tube array). The new model, christened as 'the quasi-unsteady model' to indicate both differences and similarities to the classical quasi-steady model, takes into account all of the most important unsteady effects neglected by this latter. It does so on the basis of an analysis of the behaviour of the continuity and Navier–Stokes equations, in the case of an impulsive movement of a body subject to cross-flow. This analysis is then readily extended to any arbitrary body motion using the convolution integral. Apart from the added-mass effects, the quasi-unsteady model accounts for the phenomena associated with reorganization of the flow, driven by diffusion–convection of the vorticity layer generated on the surface of the body, following each change in its velocity. This leads to unsteady terms in the fluid-dynamic forces representing an effect of memory in the flow, instead of the simple delay suggested previously by Lever & Weaver (1982) and Price & Païdoussis (1986). These terms are characterized by transient functions for which a semi-analytical modelling has been proposed, involving linear combinations of decaying exponentials. An extension of the notion of the 'flow retardation effect' has thus been achieved and a formal basis in theory has been developed for this effect.

The quasi-unsteady and Price & Païdoussis models were then compared to experimental data for square in-line and normal triangular SDOF tube arrays. These comparisons were in terms both of instability charts and of the evolution of modal parameters with flow velocity. In both cases the quasi-unsteady model provides a very satisfactory agreement with experimental data, and achieves sensibly improved theoretical prediction compared to the Price & Païdoussis model.

Analysis of the results led to the speculation that fluidelastic instability may in some cases be precipitated by an interaction with phenomena of the 'vortex shedding' type for small values of A_r (i.e. $A_r \leqslant 0.3$ approximately). Such mechanisms are not modelled by the quasi-unsteady model in its present form.

Finally, motivated by this last remark and by the question of the influence of

neighbouring-tube movements on the development of fluidelastic instability in fully flexible tube arrays, an 'experiment' was done, consisting of comparing on the same instability chart: (i) experimental data for fully flexible arrays; (ii) the results by the quasi-unsteady model for a SDOF tube array; (iii) the region where vortex shedding should occur according to the empirical correlations of Weaver & Fitzpatrick (1988). The results obtained show that (*a*) a good correlation exists between the vortex shedding zones and the critical flow velocities for fluidelastic instability for low A_r, i.e. $A_r \leqslant 1$; (*b*) a satisfactory agreement between the experimental data for flexible arrays and the single-degree-of-freedom quasi-unsteady model is obtained for $1 \leqslant A_r \leqslant 10^3$ approximately. This suggests a different interpretation of fluid–structure phenomena underlying fluidelastic instability in flexible arrays *vis-à-vis* the classical interpretation widely accepted today, which classifies the instability in terms of (i) a 'damping-controlled mechanism' for low mass-damping parameters, without reference to possible interaction with vortex shedding, and (ii) a 'stiffness-controlled mechanism' for high mass-damping parameters, essentially controlled by inter-tube motions. Of course, what has tentatively been proposed in this paragraph is only an 'exercise', not a proof. Nevertheless, the results of figure 9 should, at the very least, motivate more in-depth research in that direction.

The second author should like to acknowledge the support of NSERC of Canada and Le Fonds FCAR of Québec, and Bill Mark's assistance with some of the measurements.

REFERENCES

ANDJELIĆ, M. & POPP, K. 1989 Stability effects in a normal triangular cylinder array. *J. Fluids Struct.* **3**, 165–186.

BATCHELOR, G. K. 1967 *An Introduction to Fluid Dynamics.* Cambridge University Press.

BLEVINS, R. D. 1990 *Flow-Induced Vibration*, 2nd edition. Van Nostrand Reinhold.

CHEN, S. S. 1987 *Flow-Induced Vibration of Circular Cylindrical Structures.* Hemisphere.

CORLESS, R. M. & PARKINSON, G.V. 1988 A model of the combined effects of vortex-induced oscillation and galloping. *J. Fluids Struct.* **2**, 203–220.

FRIEDLY, J. C. 1972 *Dynamic Behaviour of Processes.* Prentice Hall.

FUNG, Y. C. 1955 *An Introduction to the Theory of Aeroelasticity.* John Wiley & Sons.

GRANGER, S. 1990 A new signal processing method for investigating fluidelastic phenomena. *J. Fluids Struct.* **4**, 73–97.

GRANGER, S., CAMPISTRON, R. & LEBRET, J. 1993 Motion-dependent excitation mechanisms in a square in-line tube bundle subject to water cross-flow: an experimental modal analysis. *J. Fluids Struct.* **7**, 521–550.

JANARDHANAN, K., PRICE, W. G. & WU, Y. 1992 Generalized fluid impulse functions for oscillating marine structure. *J. Fluids Struct.* **6**, 207–222.

KUNDU, P. K. 1990 *Fluid Mechanics.* Academic Press.

LAMB, H. 1932 *Hydrodynamics.* Cambridge University Press.

LEVER, J. H. & RZENTKOWSKI, G. 1993 Dependence of post-stable fluid-elastic behaviour on the degrees of freedom of a tube bundle. *J. Fluids Struct.* **7**, 471–496.

LEVER, J. H. & WEAVER, D. S. 1982 A theoretical model of fluid elastic instability in heat exchanger tube bundles. *Trans. ASME J. Press. Vess. Tech.* **14**, 147–158.

LEVER, J. H. & WEAVER, D. S. 1986*a* On the stability behaviour of heat exchanger tube bundles. Part 1: Modified theoretical model. *J. Sound Vib.* **107**, 375-392.

LEVER, J. H. & WEAVER, D. S. 1986*b* On the stability behaviour of heat exchanger tube bundles. Part 2: Numerical results and comparison with experiments. *J. Sound Vib.* **107**, 393–410.

LIGHTHILL, M. J. 1963 Introduction to boundary layer theory. In *Laminar Boundary Layers, Part II* (ed. L. Rosenhead), pp. 46–113. Oxford University Press.

LUO, S. C. & BEARMAN, P. W. 1990 Predictions of fluctuating lift on a transversely oscillating square-section cylinder. *J. Fluids Struct.* **4**, 219–228.

NAKAMURA, T. & FUJITA, K. 1993 An experimental study on fluid elastic vibration of a tube array by cross-flow. In *Proc. Asia-Pacific Vibration Conference 93, Symposium on FIVES, Session: Vibration of Tube Arrays*, pp. 25–30.

PAÏDOUSSIS, M. P., MAVRIPLIS, D. & PRICE, S. J. 1984 A potential flow theory for the dynamics of cylinder arrays in cross-flow. *J. Fluid Mech.* **146**, 227–252.

PAÏDOUSSIS, M. P. & PRICE, S. J. 1988 The mechanisms underlying flow-induced instabilities of cylinder arrays in cross-flow. *J. Fluid Mech.* **187**, 45–59.

PAÏDOUSSIS, M. P., PRICE, S. J., NAKAMURA, T., MARK, B. & MUREITHI, W. N. 1989 Flow-induced vibrations and instabilities in a rotated-square cylinder array in cross-flow. *J. Fluids Struct.* **3**, 229–254.

PANTON, R. L. 1984 *Incompressible Flow*. John Wiley & Sons.

PARKINSON, G. V. 1972 Mathematical models of flow-induced vibrations of bluff bodies. In *Flow-Induced Structural Vibrations* (ed. E. Naudascher), pp. 81–127. Springer.

PARKINSON, G. V. & BROOKS, N. P. H. 1961 On the aeroelastic instability of bluff cylinders. *Trans. ASME J. Appl. Mech.* **28**, 252-258.

PARKINSON, G. V. & SMITH, J. D. 1964 The square prism as an aeroelastic non-linear oscillator. *Q. J. Mech. Appl. Maths* **17**, 225–239.

PRICE, S. J. 1993 Theoretical models of fluidelastic instability for cylinder arrays subject to cross flow. In *Technology for the '90s – A Decade of Progress* (ed. M. K. Au-Yang *et al.*). ASME.

PRICE, S. J. 1995 Fluidelastic instability of cylinder arrays in cross-flow. *J. Fluids Struct.* **9**, 463–518.

PRICE, S. J. & KURAN, S. 1991 Fluidelastic stability of a rotated square array with multiple flexible cylinder subject to cross-flow. *J. Fluids Struct.* **5**, 551–572.

PRICE, S. J. & PAÏDOUSSIS, M. P. 1984*a* An improved mathematical model for the stability of cylinder rows subject to cross-flow. *J. Sound Vib.* **97**, 615–640.

PRICE, S. J. & PAÏDOUSSIS, M. P. 1984*b* The aerodynamic forces acting on groups of two and three circular cylinders when subject to a cross-flow. *J. Indust. Aero. Wind Engng* **17**, 329–347.

PRICE, S. J. & PAÏDOUSSIS, M. P. 1986 A single-flexible-cylinder analysis for the fluidelastic instability of an array of flexible cylinders in cross-flow. *J. Sound Vib.* **108**, 193–199.

PRICE, S. J. & PAÏDOUSSIS, M. P. 1989 The flow-induced response of a single flexible cylinder in an in-line array of rigid cylinders. *J. Fluids Struct.* **3**, 61–82.

PRICE, S. J. & ZAHN, M. L. 1991 Fluidelastic behaviour of a normal triangular array subject to cross-flow. *J. Fluids Struct.* **5**, 259–278.

ROBERTS, B. W. 1966 Low frequency, aeroelastic vibrations in a cascade of circular cylinders. *I. Mech. E. Mechanical Science Monograph* No. 4.

SCHWARTZ, L. 1972 *Study of Exponential Sums* (in French). Publications de l'Institut de Mathématiques de l'Université de Strasbourg, Hermann, Paris.

SEARS, W. R. 1949 *Introduction to Theoretical Hydrodynamics*. Cornell University Press.

SIMPSON, A. & FLOWER, J. W. 1977 An improved mathematical model for the aerodynamic forces on tandem cylinders in motion with aeroelastic applications. *J. Sound Vib.* **51**, 183–217.

TANAKA, H., TAKAHARA, S. & OHTA, K. 1982 Flow-induced vibration of tube arrays with various pitch-to-diameter ratios. In *Flow-Induced Vibration of Circular Cylindrical Structures* (ed. S. S. Chen, M. P. Païdoussis & M. K. Au-Yang). PVP Vol. 63, pp. 45–56. ASME.

TEH, C. E. & GOYDER, H. G. D. 1988 Data for fluidelastic instability of heat exchanger tube bundles. In *Proc. Intl Symp. on Flow-Induced Vibration and Noise*, Vol. 3 (ed. M. P. Païdoussis, S. S. Chen & M. D. Bernstein), pp. 77–94. ASME.

TELIONIS, D. P. 1981 *Unsteady Viscous Flows*. Springer.

WEAVER, D. S. & FITZPATRICK, J. A. 1988 A review of cross-flow induced vibrations in heat exchanger tube arrays. *J. Fluids Struct.* **2**, 73–93.

WEAVER, D. S., FITZPATRICK, J. A. & EL KASHLAN, M. 1986 Strouhal numbers for heat exchanger tube arrays in cross-flow. In *Flow-Induced Vibration-1986* (ed. S. S. Chen, J. C. Simonis & Y. S. Shin). PVP Vol. 104, pp. 193-200. ASME.

WEAVER, D. S. & GROVER, L. K. 1978 Cross-flow induced vibrations in a tube bank. Turbulent buffeting and fluid elastic instability. *J. Sound Vib.* **59**, 277–294.

WEAVER, D. S. & KOROYANNAKIS, D. 1982 A comparison of cross-flow induced vibration of a tube

bundle in air and water. In *Flow-Induced Vibration of Circular Cylindrical Structures* (ed. S. S. Chen, M. P. Païdoussis & M. K. Au-Yang). PVP Vol. 63, pp. 71–85. ASME.

YETISIR, M. & WEAVER, D. S. 1988 On an unsteady theory for fluid elastic instability of heat exchanger tube arrays. In *Proc. Intl Symp. on Flow-Induced Vibration and Noise*, Vol. 3 (ed. M. P. Païdoussis, S. S. Chen & M. D. Bernstein), pp. 181–195. ASME.